Model of Human Breathing Reflected Signal Received by PN-UWB Radar

Mohamed Mabrouk, Sreeraman Rajan, Miodrag Bolic, Izmail Batkin, Hilmi R. Dajani, Voicu Z. Groza

Abstract— **Human detection is an integral component of civilian and military rescue operations, military surveillance and combat operations. Human detection can be achieved through monitoring of vital signs. In this article, a mathematical model of human breathing reflected signal received in PN-UWB radar is proposed. Unlike earlier published works, both chest and abdomen movements are considered for modeling the radar return signal along with the contributions of fundamental breathing frequency and its harmonics. Analyses of recorded reflected signals from three subjects in different postures and at different ranges from the radar indicate that ratios of the amplitudes of the harmonics contain information about posture and posture change.**

Keywords— UWB radar; human breathing; displacement model

I. INTRODUCTION

Ultra wide-band (UWB) technology is gaining popularity as a non-contact methodology for monitoring vital signs. In many applications, it is necessary to monitor subject's respiration and heart rate. For example, in emergency rescue operations of burn patients, it may be impossible to measure vital signs through contact. On the other hand, with victims trapped in debris, it may be impossible to reach them, and so it may be necessary to use a non-contact monitoring approach to acquire these vital signs. Furthermore, non-contact monitoring of vital signs may be useful in long-term monitoring of the elderly as in home-care where multiple subjects may be monitored independently using a single device. Therefore, non-contact monitoring may be a viable method for improving health monitoring and reducing its costs. In military operations, non-contact monitoring may be used for security purposes by tracking subjects of interest even behind walls. For all these applications, it is necessary to model and study the process of acquiring vital signs and their associated parameters. Breathing rate and heart rate are the normally considered vital signs.

The basic idea of UWB sensing is to obtain estimates of the vital signs through signal processing of the small motions related to the organs that are responsible for producing those signs. These small motions manifest as micro-Doppler in the radar returns, which is further processed to obtain the estimates. However, depending on the carrier frequency, it may or may not be possible to obtain the heart rate as the motions related to heart are much smaller than those related to breathing.

In the literature, the signal reflected due the chest movement is often assumed to be sinusoidal [1-3], and as such is used for detecting and estimating breathing rates. In [4], human detection using movements due to breathing was investigated using periodic movements of the chest and it was concluded that movement was proportional to an absolute value of a sinusoidal signal whose frequency was the breathing frequency. A robust detection of chest motion and accurate breathing rate estimation was proposed in [5]. Modeling of the human chest was done as a multilayered medium where the electromagnetic property was assumed to be constant in each layer. Simultaneous tracking of chest respiratory rate and amplitude for sleep apnea monitoring was proposed in [6] using a 40 GHz low power ultra wide-band impulse noise radar.

Several models of movement of parts of the human body detected by the radar have been recently introduced [1-3]. The intent in those studies was to discriminate between movements of various parts of the body. Discrimination between the movements of the human chest and the arm or the wrist behind a wall using a Doppler radar system [1] was obtained using the intrinsic modes of the Doppler signatures. The extracted Doppler signatures associated with different activities were differentiated from the Doppler signature of the breathing signal which was considered as a sinusoidal signal resulting from the movements associated with the chest cavity. In [7], the human torso was considered to be of two parts and the phase variation in the wave reflected from each part was taken as a sinusoidal signal. However this was done with continuous wave radar. Recently in a population study, peak-to-peak amplitudes of the breathing displacements of several volunteers were recorded using a Real-Time Position Management (RPM) system and the mean displacement of abdomen was found to be four times that of the thorax movement [8].

Unlike the analysis presented in [9], [10] where only the chest motion is considered, this paper presents a mathematical analysis by considering the phase modulation in the radar returns due to both the thoracic and abdominal displacements. Using the new model for radar reflected signal that incorporates the thoracic and abdominal displacements due to breathing, a preliminary study with three subjects has been performed to investigate posture changes. We assume that the location of the subjects is known and the breathing rate is estimated using traditional algorithms, for example based on frequency analysis [11]. Furthermore, we assume that the target is stationary and

Mohamed Mabrouk, Sreeraman Rajan, Miodrag Bolic, Izmail Batkin, Hilmi. R. Dajani, and Viocu Z. Groza are with the University of Ottawa , ON, Canada (mmabr084@uottawa.ca, sreeraman@ieee.org, mbolic@site.uottawa.ca, vbatkin@rogers.com, hdajani@site.uottawa.ca, groza@site.uottawa.ca).

978-1-4244-7929-0/14/$26.00 ©2014 IEEE

there are no other displacements or movements. Initial results related to discriminating posture using the ratio of the amplitudes of the first and the second harmonic of the estimated breathing signal are very promising. However, these results need to be confirmed by conducting a larger study.

This paper is organized in the following manner. Section II describes the measurement setup and data collection. Section III presents the proposed model of the received signal that includes both the chest and abdomen displacements. Section IV describes the results and Section V concludes the paper.

II. Data Collection

The Pseudo Random Noise Ultra-WideBand (PN-UWB) radar is one of the most suitable technologies for detection of human life behind obstacles. It is generally non-expensive, immune to narrowband interferences, and has the ability of range gating [11]. Generally, these radars have a center frequency around 3-5 GHz and a bandwidth of about 500 MHz for high resolution [12]. A PN-UWB radar P410 produced by Time Domain Company, Huntsville, USA [13] is used in this work. The P410 radar provides a correlated output in range-bins and each range-bin is 1.907 psec which corresponds to fast time T_f. The maximum range is set to 4.38 m. The pulses obtained are integrated to provide a 36.12 dB increase in the SNR. The number of scans is 3000 and the time interval between each scan is 3.78 msec. A full scan is 16.22 ms and the time interval between each full scan (slow time) is set to T_s =20 msec to prevent overlap of the scans. The total full scan time is set to 1 minute. Figure 1 shows the P410 data collection details. The yellow cells are the range bins in the fast time direction. The slow time direction represents the scan direction and the orange spaces are the time intervals between each scan.

III. Proposed Model And Analysis

Thoracic and abdominal movements are the two important movements related to breathing. However, most of the research in human breathing detection has considered only thoracic movements in modeling the breathing signal. Only recently in [7], human breathing signal was assumed to consist of superposition of returns from thorax and abdominal movement while using continuous wave radar for Doppler-based breathing rate estimation. The human body was modeled as two cylinders, one corresponding to the thorax and the other corresponding to the abdomen with different displacements and possible phase offsets. However, the phase variation due to movements of thorax and abdomen was modeled as a sinusoid. Although [14] considered the breathing signal to be non-sinusoidal when using UWB radar, it did not explicitly analyze the signal as a combination of returns from thorax and abdomen. Interestingly in [8], it was observed that on average, the displacement of the abdomen is at least four times that of the chest; hence, it is necessary to incorporate the contributions of abdomen into the model as suggested in [7].

In this paper, the two cylinder model used in [7] along with the non-sinusoidal model proposed in [14] are adopted and new analysis is presented. Experimental observations on the spectral content of the radar returns are also presented.

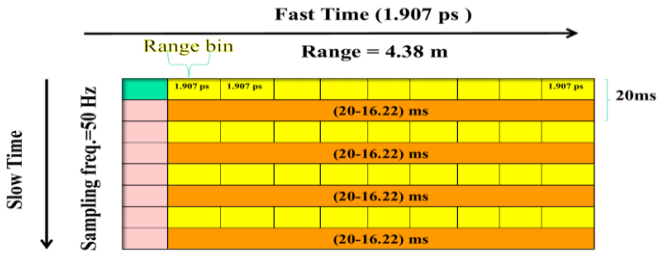

Figure 1. P410 Data collection by the P410 radar used in this study.

The signal at the receiver $d(t)$ obtained after reflecting off the chest and abdomen of a human target positioned at distance d_0 is given by

$$d(t) = d_0 + m(t) \quad (1)$$

$$= d_0 + \sum_{i=1}^{M} c_i \sin(2\pi i f_b t) + \sum_{j=1}^{N} a_j \sin(2\pi j f_b t) \quad (2)$$

where c_i are harmonic components of chest displacement and a_j are harmonic components of abdomen displacement, f_b is the breathing frequency, M and N are the number of significant harmonic components of the chest and abdomen displacements respectively. In this paper, since the radar used does not have sufficient resolution to identify heart motion, the displacement due to heart is ignored. The radar used in this study provides a correlated output. The correlated output can be represented as the sum of responses of the channel, and the variation due to chest and abdomen:

$$r(t,\tau) = \sum_i A_i p(\tau - \tau_i) + Ap(\tau - \tau_d(t)) \quad (3)$$

where $p(t)$ represents the correlation between the transmitted and received pulse, A_i is the amplitude of the correlator output which is related to the i-th static multipath component, τ_i is the time delay of the i-th static multipath, A is the amplitude of the correlator output which is related to body reflection. The time delay, $\tau_d(t)$, associated with chest and abdomen movement is modeled as sum of time-of-flight τ_0 with two composite delays as shown below:

$$\tau_d(t) = \tau_0 + \sum_{i=1}^{M} \tau_i \sin(2\pi i f_b t) + \sum_{j=1}^{N} \mu_j \sin(2\pi j f_b t) \quad (4)$$

where $\tau_0 = \frac{2d_0}{c}$, $\tau_i = \frac{2c_i}{c}$, $\mu_j = \frac{2a_j}{c}$, and c is the speed of light. The sampled correlator output is obtained at discrete instants in slow time $t = kT_s$, where T_s is the slow time sampling interval at points $k = 1, \ldots, K$ and at discrete fast sample time $\tau = lT_f$, where T_f is the fast time sampling interval at points $l = 1, \ldots, L$ and is stored as a matrix as shown in Fig. 1.

Since the environment is static, the static clutter component will appear as a DC-component in the slow-time direction and can be removed by filtering. Let the clutter free signal be $y(t,\tau)$ which contains only the movements related to chest and abdomen and is given by:

$y(t,\tau) =$
$Ap(\tau - \tau_0 - \sum_{i=1}^{M} \tau_i \sin(2\pi i f_b t) - \sum_{j=1}^{N} \mu_j \sin(2\pi j f_b t))$ (5)

If we assume that the chest movement is sinusoidal ($M = 1$) and the abdomen movement is composed of the fundamental frequency (first harmonic) and the second harmonic ($N = 2$), then the above equation becomes:

$$y(t,\tau) = Ap(\tau - \tau_0 - \tau_1 \sin(2\pi f_b t) - \mu_1 \sin(2\pi f_b t) - \mu_2 \sin(4\pi f_b t)) \quad (6)$$

The Fourier transform of $y(t,\tau)$ along the slow time can be expressed as follows:

$$Y(f,\tau) = \int_{-\infty}^{+\infty} y(t,\tau) e^{-j2\pi f t} dt \quad (7)$$

and can be obtained from the 2-D Fourier transform as follows:

$$Y(f,\tau) = \int_{-\infty}^{+\infty} Y(f,v) e^{j2\pi v \tau} dv \quad (8)$$

The 2-D Fourier transform $Y(f,v)$ can be written as follows

$$Y(f,v) = AP(v) e^{-j2\pi v \tau_0} \int_{-\infty}^{+\infty} (S_1 S_2 S_3) e^{-j2\pi f t} dt \quad (9)$$

where $P(v)$ is the Fourier transform in the fast time of the correlated pulse and:

$$S_1 = \sum_{k=-\infty}^{+\infty} J_k(\beta_{\tau_1} v) e^{-j2\pi k f_b t} \quad (10)$$

$$S_2 = \sum_{l=-\infty}^{+\infty} J_l(\beta_{\mu_1} v) e^{-j2\pi l f_b t} \quad (11)$$

$$S_3 = \sum_{m=-\infty}^{+\infty} J_m(\beta_{\mu_2} v) e^{-j2\pi m(2f_b) t} \quad (12)$$

where $\beta_x = 2\pi x$ and $\sum_{p=-\infty}^{+\infty} J_p(z) e^{-j2\pi p f_0 t} = e^{-jz\sin(2\pi f_0 t)}$ is the series of Bessel functions.

After substituting and simplifying, it can be shown that at $\tau = \tau_0$

$$Y(f,\tau_0) = A \sum_{k,l,m=-\infty}^{+\infty} C_{klm} \delta(f - (k+l)f_b - m(2fb)) \quad (13)$$

where

$$C_{klm} = \int_{-\infty}^{+\infty} P(v) J_k(\beta_{\tau_1} v) J_l(\beta_{\mu_1} v) J_m(\beta_{\mu_2} v) dv$$

Furthermore using the mean value theorem C_{klm} can be evaluated as follows [15]:

$$C_{klm} \approx \Delta f . J_k(\beta_{\tau_1} f_c) J_l(\beta_{\mu_1} f_c) J_m(\beta_{\mu_2} f_c) P(f_c) \quad (14)$$

where Δf is the pulse bandwidth. The above equation indicates the slow time spectrum is discrete and has spectral lines at frequencies of the harmonics of the breathing frequency. These harmonics are intermodulation products of the chest and abdomen movements. The amplitude of each intermodulation product at a given frequency $f = (k+l)f_b + m2f_b$ is determined by the coefficient C_{klm} . It may be noted that the modulation index β_x in (14) changes with the posture as the abdomen and chest displacements are different for different postures. As a consequence, the values of the coefficients C_{klm} change with posture. This information can be effectively used to identify the posture of the target or at the least provide an indication of possible posture of the target. The coefficient at the breathing frequency is given by $C_f = C_{100} + C_{010}$ while the coefficient at the second and the third harmonics are respectively given by $C_{2f} = C_{001} + C_{200} + C_{020} + C_{110}$ and $C_{3f} = C_{300} + C_{030} + C_{101} + C_{011} + C_{210} + C_{120}$. The ratio of the harmonics, $R_{21} = \frac{C_{2f}}{C_f}$ and $R_{31} = \frac{C_{3f}}{C_f}$ will vary with posture and by estimating these ratios, it may be possible to identify the posture of the target.

IV. Results

In this work, the target's location is either given or assumed to be already correctly estimated and the focus is on obtaining the value of the ratios R_{21} and R_{31} for various postures to demonstrate the fact that they contain information about the posture of the target.

Measurements were obtained from three targets lying on their back, sitting, and standing in free space 1 m, 2 m and 3 m from the P410 PN-UWB radar. The subjects were asked to take a breath when they heard a tone generated by a software program. The tone was repeated every 3.33 seconds. The measurement protocol was approved by the University of Ottawa Research Ethics Board. The subjects wore a breathing belt produced by CleveMed ™, Cleveland, USA during every measurement and was used to confirm that the breathing rate was same for all measurements (18 ± 1 breaths/min).

The correlator output data was obtained as a data matrix (see Fig. 1). The out-of-band frequencies in the fast time was removed by using a 16th order infinite impulse response (IIR) Butterworth Band-pass filter (BPF) with transition band from 3.1 to 5.1 GHz. The stationary clutter was removed using a moving target indicator filter, essentially a high pass filter [16]. Since the target's position was known, the slow time waveform at the bin corresponding to the location of the target was used for further processing. This waveform was obtained at a sampling frequency of 50 Hz and was filtered using a 6th order IIR Butterworth BPF from 0.1-1 Hz. The spectrum of the filtered waveform was obtained using the Fast Fourier transform (FFT). The first prominent peak location, $\hat{f}_b$, close to f_b, in the spectrum, is considered as the breathing frequency and its amplitude is taken as C_f. Then the second and third prominent peak locations, which should be close to $2\hat{f}_b$ and $3\hat{f}_b$ are taken as $\hat{f}_{2b}$ and $\hat{f}_{3b}$, and their amplitudes are taken as C_{2f} and C_{3f}, respectively. The ratios R_{21} and R_{31} are calculated for each posture of the target at a given distance.

Table I shows the results over several trials. It is clear from the table that amongst ratios of amplitude harmonics for the three postures (sitting, standing and lying down), R_{21} is the highest while stitting while R_{31} is the lowest while lying

down. The amplitude of the second harmonic is 1.4 times higher on an average than the amplitude of the fundamental frequency while sitting. On the other hand, the amplitude of the second harmonic is 0.8 and 0.56 times the amplitude at the fundamental frequency for standing and supine positions respectively. Similar observations can be made for the third harmonic. Thus, change in the posture affects the ratios and can be used to identify changes in posture. Figure 2 shows the FFT of the received signal of a subject sitting and lying supine 2 m from the radar, respectively and breathing at 0.3 Hz rate. The radar was placed directly in front of the subject in both cases. The figure clearly indicates the spectral differences due to posture. However, in order to identify the postures themselves, these ratios may be sometimes inadequate as the distribution of these ratios may have substantial overlap. Hence it may be necessary to identify further features of the spectral pattern to classify postures.

TABLE I. RATIO OF THE AMLITUDES OF THE HARMONICS.

Subject	Distance	*Standing*		*Sitting*		*Lying down*	
		R_{21}	R_{31}	R_{21}	R_{31}	R_{21}	R_{31}
A	1m	0.57	0.25	1.6	0.6	1	0.24
B	1m	0.6	0.27	0.6	0.1	0.33	0.05
C	1m	0.5	0.54	1.53	0.53	0.9	0.3
A	2m	0.8	0.3	1.8	0.45	0.3	0.08
B	2m	1.1	0.38	1	0.5	0.4	0.25
C	2m	1.29	0.27	1	0.25	0.72	0.08
A	3m	1.5	0.47	1.33	0.55	0.3	0.08
B	3m	0.4	0.35	2.57	1.5	0.4	0.25
C	3m	0.4	0.18	1.17	0.29	0.7	0.08
Mean ratio		**0.80**	**0.34**	**1.40**	**0.53**	**0.56**	**0.16**
Standard division		**0.41**	**0.11**	**0.57**	**0.39**	**0.27**	**0.09**

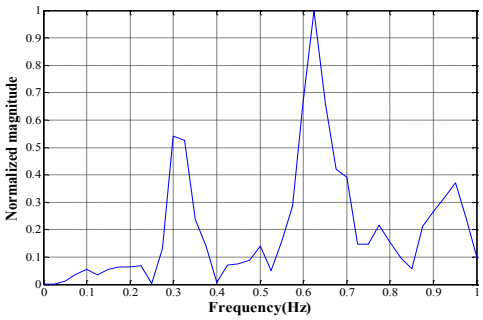

(a)

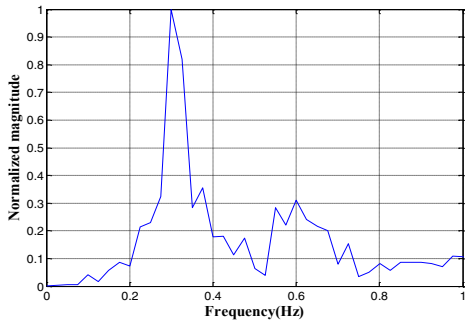

(b)

Figure 2. FFT of the signal reflected from a target (a) Sitting 2 m from the radar. (b) Lying on his back 2 m from the radar.

V. CONCLUSION

In this paper, we proposed a new mathematical model of human breathing reflected signal received in PN-UWB radar that explicitly incorporated the chest and abdomen displacement. This model can be used to better understand the chest/abdomen movements in relation to posture. The ratios of the amplitude of the harmonics may be used as features for classification of the target's posture. Future work will focus on detection of posture changes and classification of postures while detecting a human behind a wall.

REFERENCES

[1] R. M. Narayanan *et al.,* "Through-the Wall Detection of Stationary Human Targets Using Doppler Radar," *Progress in Electromagnetics Research B*, vol. 20, pp. 147-166, 2010.

[2] P. Van and F. Groen, "Human walking estimation with radar," *IEE Proc. Radar, Sonar, and Navigation*, vol. 150, no. 5, pp. 356-365, 2003.

[3] S. Gürbüz, "Radar detection and identification of human signatures using moving platforms," PhD. Dissertation, Georgia Institute of Technology, Georgia, Atlanta, 2009.

[4] A. Nezirovic, A.G. Yarovoy and L.P Ligthart, "Experimental study on human being detection using UWB radar," *International Radar Symposium*, 2006, pp. 1-4.

[5] Y.Chen and P. Rapajic, "Human respiration rate estimation using ultra-wideband distributed cognitive radar system," *International Journal on Automation and Computing*, vol. 5, issue 4, pp. 325-333, Oct 2008.

[6] J. C.Y. Lai *et al*., "Wireless Sensing of Human Respiratory Parameters by Low-Power Ultrawideband Impulse Radio Radar," *IEEE Trans. Inst. Meas.*,vol 60, no. 3, pp. 928-938, March 2011.

[7] J. E. Kiriazi *et al*., "Modeling of human torso time-space characteristics for respiratory effective RCS measurements with Doppler radar," *IEEE International Microwave Symposium Digest* (*MTT*), Baltimore, MD, 2011, pp. 1-4.

[8] S. Quirk *et al*.,"External Respiratory Motion Analysis and Statstics for Patients and Volunteers," *Journal of Applied Clinical Medical Physics*, vol. 14, no. 2, pp. 90-101, 2013.

[9] J. Li *et al.*, "Through-Wall Detection of Human Being's Movement by UWB Radar," *IEEE Geosci. Remote Sens. Lett*., vol. 9, no. 6, pp. 1079-1083, Nov. 2012.

[10] L. Liu *et al*., "Through-Wall Bio-Radiolocation with UWB Impulse Radar: Observation, Simulation and Signal Extraction," *IEEE J. of Selected Topics in Appl. Earth Observations and Remote Sens*., vol. 4, no. 4, pp. 791-797, Dec. 2011.

[11] J. Li *et al.*, "Through-Wall Detection of Human Being's Movement by UWB Radar," *IEEE Geosci. Remote Sens. Lett*., vol. 9, no. 6, pp. 1079- 1083, Nov. 2012.

[12] S. Singh *et al.* "Sense Through Wall Human Detection Using UWB Radar," *Journal on Wireless Communications and Networking* (*EURASIP*), pp. 1-11, 2011.

[13] Time Domain (2013, Oct. 31), PulsON®410, P410 radar kit, [Online]. Available: http://www.timedomain.com/.

[14] S. Venkatesh *et al*.," Implementation and analysis of respiration-rate estimation using impulse-based UWB," *IEEE Military Communications Conference* (*IEEE Milcom'05*), vol. 5, Oct. 2005, pp. 3314-3320.

[15] A. Lazaro *et al.*, "Analysis of Vital Signs Monitoring Using an IR-UWB Radar," *Electromagnetics Research*, PIER, pp. 265-284, 2010.

[16] M. Mabrouk *et al*.,"Detection of Human Targets behind the Walls Based on Singular Value Decombosition and Skewness Variations," *2014 IEEE Radar Conference*, Cincinnati, OH, 2014, pp. 1466-1470.